# The Fer Tyrosine Kinase Cooperates with Interleukin-6 to Activate Signal Transducer and Activator of Transcription 3 and Promote Human Prostate Cancer Cell Growth

**Amina Zoubeidi,[1,2] Joice Rocha,[1] Fatima Z. Zouanat,[1] Lucie Hamel,[1] Eleonora Scarlata,[1] Armen G. Aprikian,[1] and Simone Chevalier[1,2]**

*[1]Urologic Oncology Research Group, Departments of Surgery (Urology Division), Medicine, and Oncology, McGill University Health Center Research Institute; [2]Department of Biochemistry, University of Montreal, Montreal, Quebec, Canada*

## Abstract

**Androgen withdrawal is the most effective form of systemic therapy for men with advanced prostate cancer. Unfortunately, androgen-independent progression is inevitable, and the development of hormone-refractory disease and death occurs within 2 to 3 years in most men. The understanding of molecular mechanisms promoting the growth of androgen-independent prostate cancer cells is essential for the rational design of agents to treat advanced disease. We previously reported that Fer tyrosine kinase level correlates with the development of prostate cancer and aggressiveness of prostate cancer cell lines. Moreover, knocking down Fer expression interferes with prostate cancer cell growth *in vitro*. However, the mechanism by which Fer mediates prostate cancer progression remains elusive. We present here that Fer and phospho-Y705 signal transducer and activator of transcription 3 (STAT3) are barely detectable in human benign prostate tissues but constitutively expressed in the cytoplasm and nucleus of the same subsets of tumor cells in human prostate cancer. The interaction between STAT3 and Fer was observed in all prostate cancer cell lines tested, and this interaction is mediated via the Fer Src homology 2 domain and modulated by interleukin-6 (IL-6). Moreover, IL-6 triggered a rapid formation of Fer/gp130 and Fer/STAT3 complexes in a time-dependent manner and consistent with changes in Fer and STAT3 phosphorylation and cytoplasmic/nuclear distribution. The modulation of Fer expression/activation resulted in inhibitory or stimulatory effects on STAT3 phosphorylation, nuclear translocation, and transcriptional activation. These effects translated in IL-6–mediated PC-3 cell growth. Taken together, these results support an important function of Fer in prostate cancer. (Mol Cancer Res 2009;7(1):142–55)**

## Introduction

The earlier detection of prostate cancer has had significant effect on the management of localized disease by active surveillance, surgery, or radiation therapy. However, therapeutic options for non–organ-confined prostate cancer remain primarily noncurative and hormone based. In most instances, patients successfully respond to androgen ablation (1), but eventually, a majority of them fail and progress to the hormone-refractory stage (2). This represents a major obstacle for cure because at this point no effective therapy exists. As such, prostate cancer remains a major cause of death from cancer in several industrialized countries. Progression is a highly complex process that is not fully understood. Recent studies indicate that prostate tumor cells develop alternative mechanisms to grow, and notably respond to diverse growth factors that activate associated regulatory molecules required for signaling (3-5). Among others, accumulating data point out to the importance of tyrosine kinases in the evolution of prostate cancer. Hence, the development of small inhibitory drugs targeting tyrosine kinases, such as gefitinib and imatinib, for the intrinsic enzymes of the epidermal growth factor receptor (6) and platelet-derived growth factor receptor (7), respectively, has opened a new window for therapeutic interventions. Although enthusiasm for these approaches remains high, prostate tumor heterogeneity and, importantly, redundancy in signaling pathways dictate the need to better understand central mechanisms linking tyrosine kinases to tumor growth to discover new therapeutic targets.

Fer is a 94-kDa nonreceptor tyrosine kinase structurally characterized by a central Src homology 2 (SH2) and COOH-terminal tyrosine kinase domains, distinguished from members of the Src, Abl, Btk, Janus-activated kinase (JAK), Zap70, or Fak cytoplasmic tyrosine kinase subfamilies by an $NH_2$-terminal FER/ClP4 homology and adjacent coiled-coil domains (8, 9) forming ECF domain in PCH adaptor proteins (10). Although a role of Fer in oncogenesis has been proposed, underlying molecular mechanisms remain unclear. We previously

Received 2/28/08; revised 8/29/08; accepted 9/23/08.
**Grant support:** Cancer Research Society, Inc. and Department of Urology, McGill University Health Center. A. Zoubeidi and J. Rocha received studentships from the Department of Biochemistry, Faculty of Graduate Studies, Montreal University, and the McGill Urology Division and McGill University Health Center Research Institute, respectively.
The costs of publication of this article were defrayed in part by the payment of page charges. This article must therefore be hereby marked *advertisement* in accordance with 18 U.S.C. Section 1734 solely to indicate this fact.
**Note:** J. Rocha is the first coauthor.
**Requests for reprints:** Simone Chevalier, McGill University Health Center Research Institute, 1650 Cedar Avenue, Montreal, Quebec, Canada H3G 1A4. Phone: 514-934-1934, ext. 44616; Fax: 514-934-8261. E-mail: simone.chevalier@mcgill.ca

doi:10.1158/1541-7786.MCR-08-0117

reported that Fer is a highly expressed protein kinase in human prostate cancer tissue extracts in comparison with normal or benign organs (11). Interestingly, Fer localized in both the cytoplasmic and nuclear compartments of prostate cancer cells and brain tumor cells (11-14). In addition, the stable down-regulation of Fer using antisense cDNA impairs PC-3 cell growth and colony formation *in vitro* (11). RNA interference against Fer similarly inhibits cell proliferation, causing a $G_0$-$G_1$ cell cycle arrest via the retinoblastoma protein, cyclin-dependent kinases (CDK4 and CDK2), and phosphatase PP1α (15).

Fer is implicated in signaling pathways activated by growth factors, such as epidermal growth factor and platelet-derived growth factor (16). It also regulates the cytoskeleton through an interaction with phosphorylated cortactin via its SH2 domain (17). Fer has been reported to interact with the signal transducer and activator of transcription 3 (STAT3; ref. 18) and with phosphatidylinositol 3-kinase in insulin signaling, thereby suggesting a role in cell survival (19). Furthermore, Fer dominant negative was shown to interfere with STAT3 phosphorylation in CHO and COS cells (18). This connection of Fer with STAT3 is particularly attractive in the context of prostate cancer. Indeed, interleukin-6 (IL-6) now figures as a surrogate marker for androgen-independent prostate cancer in conjunction with activated STAT3 (20). The STAT3 signalosome is thus determinant for progression of the disease. However, very little is known on the regulation of STAT3 activation in the IL-6 pathway in androgen-independent prostate cancer cells.

Here, we report that Fer and phospho-Y705 STAT3 (pSTAT3) are coexpressed in both the cytoplasm and nucleus of human prostate cancer specimens. Moreover, Fer and pSTAT3 interact in different prostate cancer cell lines, and this interaction is specifically mediated via the Fer-SH2 domain. Fer also forms complexes with the IL-6 receptor gp130. Furthermore, Fer is required for IL-6 signaling that regulates STAT3 phosphorylation, nuclear translocation, and transcriptional activation and then modulates cell growth. These novel findings point to a novel role of the Fer tyrosine kinase in prostate cancer progression by regulation of STAT3 transcriptional activity.

## Results

### *Fer and pSTAT3 Expression and Colocalization in Human Prostate Cancer Tissues*

We reported that Fer protein levels correlate with the development of prostate cancer and aggressive properties of prostate cancer cell lines (11). Similarly, STAT3 expression correlates with prostate cancer progression (21, 22). Because Fer and STAT3 interact in different cell model systems, we attempted to determine if Fer and STAT3 were coexpressed in human prostate cancer. First, the expression of Fer in the human prostate was investigated using homemade Fer antibodies raised against the $NH_2$-terminal domain of Fer fused to glutathione *S*-transferase (GST). As shown in Fig. 1A, Fer antibodies recognized a major band at 94 kDa, which was displaced by preincubation of antibodies with increasing amounts of purified Fer-GST protein. Furthermore, Fer antibodies had the ability to specifically immunoprecipitate ectopically expressed Fer in PC-3 cells, with recombinant myc-Fer being recognized using myc antibodies. By immunofluorescence, Fer antibodies revealed a cytoplasmic and nuclear subcellular localization of the protein in PC-3 cells grown in 10% serum (Fig. 1A, *top right*), whereas preimmune immunoglobulins (IgG) failed to show any staining (data not shown). Such a distribution is consistent with earlier fractionation studies (11). In addition, the signal was markedly diminished once Fer was knock down using *fer* small interfering RNA (siRNA; Fig. 1A, *bottom*), implying specificity. Fer antibodies did not cross-react with its homologue Fes, found in T cells but not in prostate cancer cells (data not shown).

To establish a relationship between Fer and STAT3 in human prostate cancer, specimens were stained with both Fer and STAT3 antibodies. Figure 1B (*left*) shows that within the same specimen, Fer was predominantly expressed in tumor cells compared with benign glandular cells, confirming an up-regulation of Fer and suggesting a role in human prostate cancer. In agreement with earlier reports (22), STAT3 antibodies revealed expression in both normal and malignant prostates (Fig. 1B, *middle*). Based on Fer activation of STAT3 by Y705 phosphorylation (pSTAT3; ref. 18), phosphotyrosine-specific STAT3 antibodies were then used to investigate pSTAT3 staining along with Fer in prostate tissues. Figure 1B (*right*) shows weak pSTAT3 antibodies immunoreactivity in benign glands and a strong signal resembling that of Fer in both the cytoplasm and nucleus of prostate tumor cells. A pilot study was thus conducted on a small subset of 21 prostate cancer specimens to explore any further potential links between Fer and pSTAT3. Representative photomicrographs of both Fer and pSTAT3 staining on consecutive sections are shown in Fig. 1C. Overall, most sections were positively expressing Fer (76%) and pSTAT3 (67%). In positive cases, over 94% in the two subcategories were advanced disease or high pathologic Gleason score (≥8). Fer and pSTAT3 were coexpressed in the cytoplasm (Fer, 72%; pSTAT3, 67%) and nucleus (Fer, 62%; pSTAT3, 67%) of prostate tumor cells, and their distribution was not statistically different (cytoplasm $P = 0.35$; nucleus $P = 0.75$). Results summarized in Table 1 indicate that both cytoplasmic and nuclear Fer and pSTAT3 were elevated in Gleason score 10 in comparison with Gleason 6 to 7 ($P < 0.05$). The relative staining intensity for both Fer and pSTAT3 antibodies varied from faint (+) to moderate (++) and strong (+++) and was equal or stronger in the nucleus comparatively with the cytoplasmic signal in ~90% of cases. These findings on Fer are consistent with our earlier report on high expression levels detected on Western blots of human prostate cancer tissue extracts (11). This suggests that Fer expression levels and distribution in the cytoplasm and nucleus in subsets of tumors vary along with pSTAT3, which is elevated in advanced disease (21, 23).

### *Fer Forms Complexes with STAT3 in Prostate Cancer Cell Lines*

Fer has been reported to interact with STAT3 in different cell systems (18, 19, 24). Because Fer and pSTAT3 seemed to be expressed in the same subcellular compartments in subsets

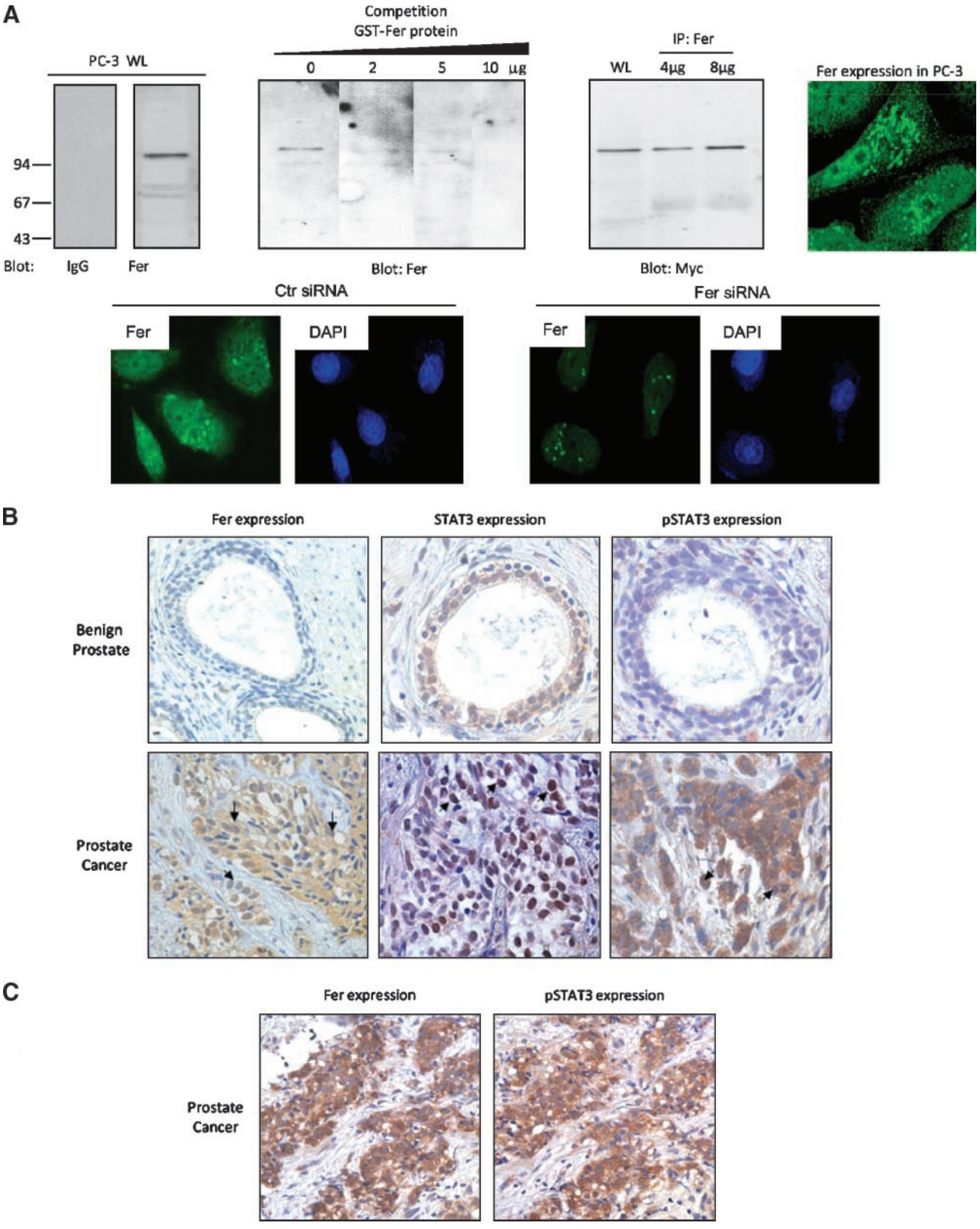

**Table 1. Fer and pSTAT3 Expression and Distribution in Human Prostate Cancer According to Gleason Score**

| Gleason score ($n$ = 21) | Fer | | | | pSTAT3 | | | |
|---|---|---|---|---|---|---|---|---|
| | 6 and 7 ($n$ = 5) | 8 ($n$ = 3) | 9 ($n$ = 8) | 10 ($n$ = 5) | 6 and 7 ($n$ = 5) | 8 ($n$ = 3) | 9 ($n$ = 8) | 10 ($n$ = 5) |
| Cytoplasm staining (%) | 4 ± 9 | 16 ± 22 | 30 ± 28 | 48 ± 5* | 0 ± 0 | 23 ± 21 | 21 ± 22 | 32 ± 48* |
| Nucleus staining (%) | 0 ± 0 | 77 ± 12 | 70 ± 30 | 90 ± 0* | 0 ± 0 | 50 ± 44 | 70 ± 32 | 86 ± 5* |

*Statistically different ($P < 0.05$) from Gleason 6 to 7.

of tumor cells of prostate cancer specimens (Fig. 1B and C; Table 1), we tested the presence of Fer/STAT3 complexes in human PC-3 cells. Figure 2 shows that Fer and STAT3 were recovered in both Fer (Fig. 2A, *left*) and STAT3 (Fig. 2A, *middle*) immunoprecipitates, suggesting that Fer and STAT3 strongly interact. Similar Fer/STAT3 complexes were found in other human prostate cancer cell lines, such as LNCaP, PRO4, and DU145 (Fig. 2A, *right*), thereby suggesting no particular relationship of Fer/STAT3 complexes with androgen sensitivity and implying that they may be important in prostate cancer.

### *Fer Is a Partner of IL-6 Signaling Molecules in Prostate Cancer Cells*

Approximately 50% of patients with advanced prostate cancer have elevated levels of serum IL-6 in comparison of men with normal prostates, benign prostatic hyperplasia, and localized disease (20, 25). In addition, IL-6 has been associated with progression from hormone-sensitive to hormone-insensitive disease in animal models via interaction with androgen receptor (AR) cofactors (26). Basically, IL-6 binds to its cognate α-chain receptor (IL-6 receptor) with low affinity, and then the complex binds to the signal-transducing molecule gp130 (β-subunit) to form a high-affinity complex (27). IL-6 induces rapid phosphorylation of gp130; this phosphorylation can be induced by JAKs or Fes tyrosine kinases and triggers the signaling cascade leading to STAT3 phosphorylation, dimerization and nuclear translocation, and action at the gene level (28, 29). Because Fer interacts with STAT3 in PC-3 cells, we investigated if this complex is modulated by IL-6. As shown in Fig. 2B (*left*), we found that IL-6 induced Fer/STAT3 complexes with a maximal level at 30 minutes without affecting levels of Fer and STAT3 proteins. Interestingly, the extent of Fer interaction with phospho-activated STAT3 (Fig. 2B, *right*) increased when Fer was also activated by tyrosine phosphorylation. Taken together, these data showed that higher levels of Fer/STAT3 complexes exist when they are phospho-activated by IL-6.

To provide further insight on this signaling pathway involving Fer activation by IL-6, we dissected the Fer tyrosine phosphorylation pattern in a time-dependent manner. IL-6 induced Fer tyrosine phosphorylation within 5 minutes (Fig. 2C), suggesting the possibility that Fer could be involved with IL-6 receptor (gp130) similarly to its homologue Fes (28). Given the expression of gp130 in PC-3 cells (30), we investigated whether Fer may be involved early in IL-6 signaling (i.e., at the receptor level). Therefore, the possibility of Fer forming a complex with gp130 was examined by probing reciprocal blots of gp130 and Fer immunoprecipitates with antibodies to detect Fer and gp130, respectively. Figure 2D confirms the existence of specific endogenous gp130/Fer complexes and also illustrates the migration position of Fer and gp130 in whole-cell lysates. Furthermore, gp130/Fer complexes were modulated by IL-6 in parallel with gp130 tyrosine phosphorylation and without affecting levels of gp130 and Fer expression (Fig. 2D, *right*). Altogether, these data showed that Fer is a part of IL-6/gp130/pSTAT3 signaling pathway.

### *Fer Phosphorylates STAT3*

It has been reported that overexpression of Fer in COS cells increases STAT3 tyrosine phosphorylation (18). We tested whether Fer activity may determine the status of STAT3 activation. For this purpose, the recombinant myc-tagged double-mutant (DM)-Fer protein (cDNA mutated in the catalytic domain and lacking the autophosphorylation site) versus wild-type (WT)-Fer was overexpressed in PC-3 cells and STAT3 phosphorylation was evaluated. STAT3 antibodies revealed similar levels of STAT3 in PC-3 cells overexpressing either WT-Fer or DM-Fer (Fig. 3A). In contrast, phosphotyrosine-STAT3 antibodies indicated that STAT3 activation was largely impaired. Consistent with findings in COS cells showing that dominant-negative Fer hampers STAT3 function (18, 24), these results also suggest that Fer is an important enzyme activating STAT3 in PC-3 cells. Next, we asked whether Fer tyrosine kinase phosphorylates STAT3 directly.

**FIGURE 1.** Fer and STAT3 expression and localization in human prostate cancer. **A.** Specificity of Fer antibodies: IgGs purified from preimmune (IgG) and immune (Fer) rabbit sera were tested for their ability to detect Fer in PC-3 cells. Top left, Western blotting with Fer antibodies (1:3,000, 1 h) and preimmune IgGs (1:3,000, 1 h) showing the 94-kDa Fer protein relative to the position of molecular markers in whole-cell lysates (*WL*). First middle, to assess specificity, Fer antibodies were preincubated in the presence of 0, 2, 5, and 10 μg of GST-Fer fusion protein for 15 min at room temperature before Western blotting; second middle, the recombinant Fer protein was immunoprecipitated from PC-3 cells transfected with WT-*fer* cDNA tagged with a myc-his epitope using 4 and 8 μg of Fer antibodies and detected by Western blotting using myc antibodies (1:5,000, 1 h). Right, photomicrograph showing Fer expression and distribution in fixed PC-3 cells by immunofluorescence once stained with Fer antibodies. Bottom, Fer expression in PC-3 cells after a 2-d treatment with siRNAs. Left, control; right, *fer* sequence 1. Fer is shown and DAPI counterstaining to delineate the nucleus. Magnification, ×400. **B.** Immunohistochemical staining to detect Fer, STAT3, and pSTAT3 expression in human prostate tissues. Left, Fer antibodies (1:25 dilution or 4 μg/mL); middle, STAT3 antibodies (1:100 dilution); right, pSTAT3 antibodies (1:100 dilution). Photomicrographs showing staining for each protein in tumor foci (*bottom rows*) and benign glands (*top rows*) in a representative prostate cancer specimen. Magnification, ×400. **C.** Representative photomicrographs of Fer (*left*) and pSTAT3 (*right*) in human prostate cancer from a series of 21 back to back slides immunostained with Fer along with pSTAT3 antibodies. Magnification, ×400.

*In vitro* phosphorylation assays were done in the presence of radiolabeled [γ-$^{32}$P]ATP using catalytic domains of human and mouse Fer as source of active enzymes. A pSTAT3 peptide was added in parallel as a potential Fer inhibitor and competitor for this motif in the STAT3 substrate. Figure 3B (*top*) revealed two radiolabeled bands corresponding to predicted sizes of 59 to 60 kDa for Fer catalytic domains and 120 kDa for STAT3. Similar results were obtained with human and mouse Fer. No

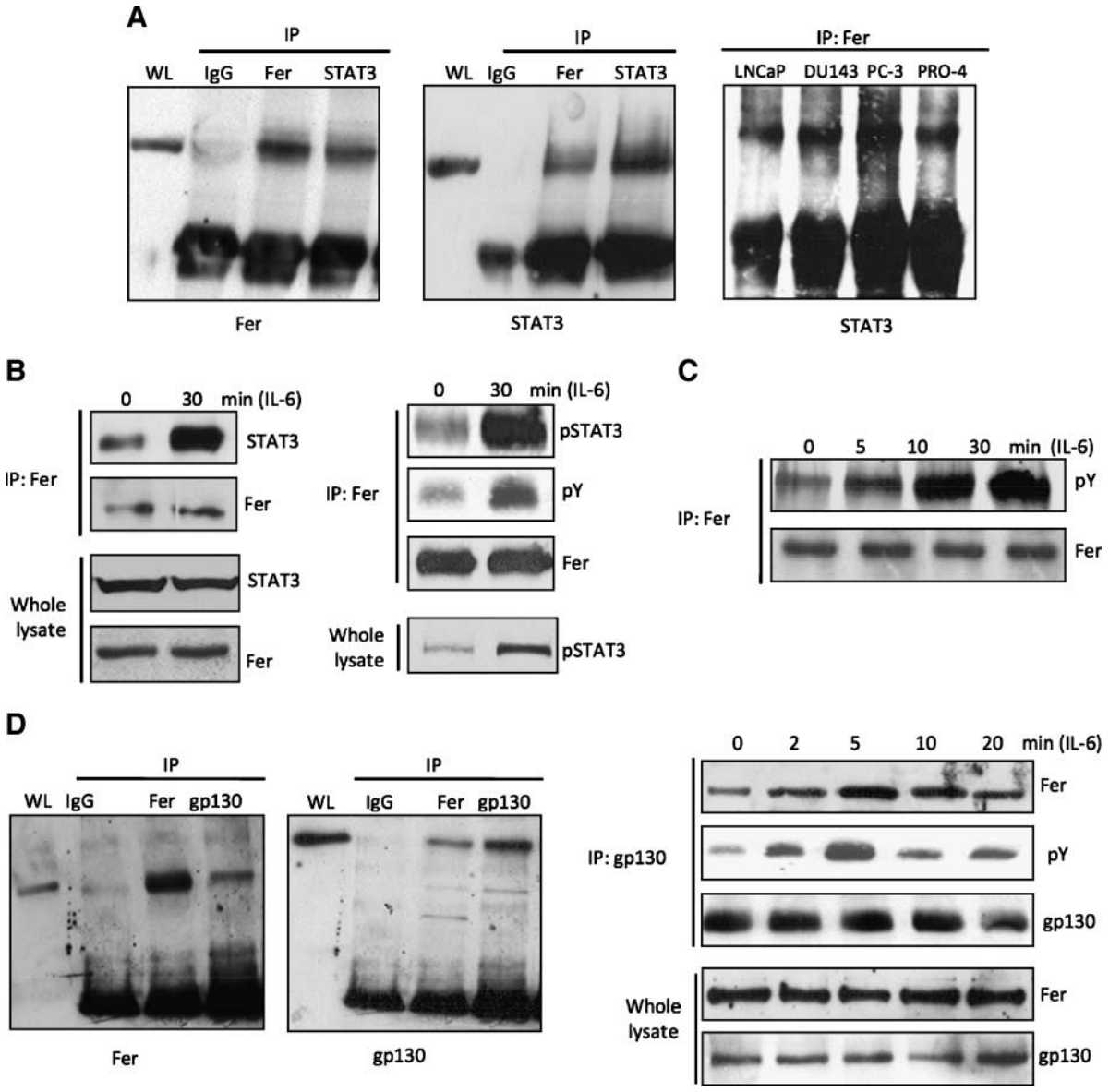


**FIGURE 2.** Fer forms complexes with STAT3 and gp130 in an IL-6–dependent manner. **A.** Fer/STAT3 complexes in prostate cancer cell lines. Top, whole PC-3 cell lysates (750 μg proteins) were immunoprecipitated with 2 μg control IgG, Fer, and STAT3 antibodies and blotted to detect Fer (1:3,000 for 1 h; *left*) or STAT3 (1:1,000 overnight; *middle*). Fer and STAT3 in whole-cell lysates (30 μg proteins in *left lanes*) are shown. Whole lysates (750 μg proteins) from LNCaP, DU145, PC-3, and variant PRO4 cells were immunoprecipitated with Fer antibodies and blotted with STAT3 antibodies as above. **B.** Fer complexes with STAT3 and pSTAT3 are IL-6 dependent, right. PC-3 cells were serum starved for 48 h before stimulation with IL-6 for 30 min. Left, top, proteins (750 μg) were immunoprecipitated with Fer antibodies and blotted with either STAT3 or Fer antibodies; bottom, whole-cell lysates (30 μg proteins) were used to monitor the expression of STAT3 and Fer. Right, top, PC-3 cells were stimulated with IL-6 and Fer was immunoprecipitated for subsequent blotting with either pSTAT3 antibodies, phosphotyrosine (*pY*) antibodies (1:3,000 for 1 h) to monitor Fer activation, or Fer antibodies as a control of immunoprecipitation; bottom, levels of pSTAT3 were measured in parallel by direct blots of whole-cell lysates with pSTAT3 antibodies. **C.** Fer is rapidly activated by IL-6. PC-3 cells were stimulated with IL-6 over time. Fer was immunoprecipitated from cell lysates for subsequent blotting with phosphotyrosine antibodies (1:3,000 for 1 h) or Fer antibodies as a control of immunoprecipitation. **D.** Fer forms complexes with gp130 in an IL-6–dependent manner. Left, whole PC-3 cell lysates (750 μg proteins) were immunoprecipitated with 2 μg control IgG, Fer, and gp130 antibodies and Western blotted for 1 h to detect Fer (1:3,000) or gp130 (1:2,000). Fer and gp130 in whole-cell lysates (30 μg proteins in *left lanes*) are shown. Right, IL-6 regulates Fer complexes with gp130 and gp130 activation in prostate cancer cells. Immunoprecipitation from lysates of PC-3 cells stimulated with IL-6 over time was carried out with gp130 antibodies. Blots were probed with antibodies to detect Fer (*first panel*) and phosphotyrosine (*second panel*) showing complexes and gp130 activation. Equal levels of gp130 in gp130 immunoprecipitates (*third panel*) and of Fer (*fourth panel*) and gp130 (*fifth panel*) in whole-cell lysates are shown.

120-kDa labeled band was seen when omitting Fer catalytic domains and only one 60 kDa labeled band was detected in the control with enzyme alone. This implies that in these conditions, Fer phosphorylates STAT3 and is also capable of autotransphosphorylation. The radiolabeling of STAT3 at 120 kDa was largely reduced in the presence of STAT3 inhibitor peptide, implying that Y705 is phosphorylated. This STAT3 peptide seemed to affect the labeling of mouse but not human Fer, apparently loaded equally in gels as seen after Coomassie blue staining (Fig. 3B, *bottom*). STAT3 was identified by Western blots with STAT3 antibodies as a 120-kDa protein in all lanes, except in the control containing no STAT3 substrate (Fig. 3B, *left middle*). The STAT3 phosphorylation status at Y705 was confirmed in parallel blots using pSTAT3 antibodies and detecting the 120-kDa immunoreactive band in complete assays where both Fer and STAT3 were present. This band was not seen in control lanes with Fer or STAT3 alone (Fig. 3B, *right middle*), implying specificity. Taken together, these data are in support of active Fer directly controlling the phosphorylation status of STAT3 on Y705 residue.

Because Fer phosphorylates STAT3 directly and Fer contains a SH2 domain, we hypothesized that Fer interacts with STAT3 via its SH2 domain and tyrosine phosphorylated STAT3. To test this possibility, a Fer-SH2-GST fusion protein and control GST protein were generated to do pull-down assays from PC-3 cell extracts exposed or not to IL-6 for 30 minutes.



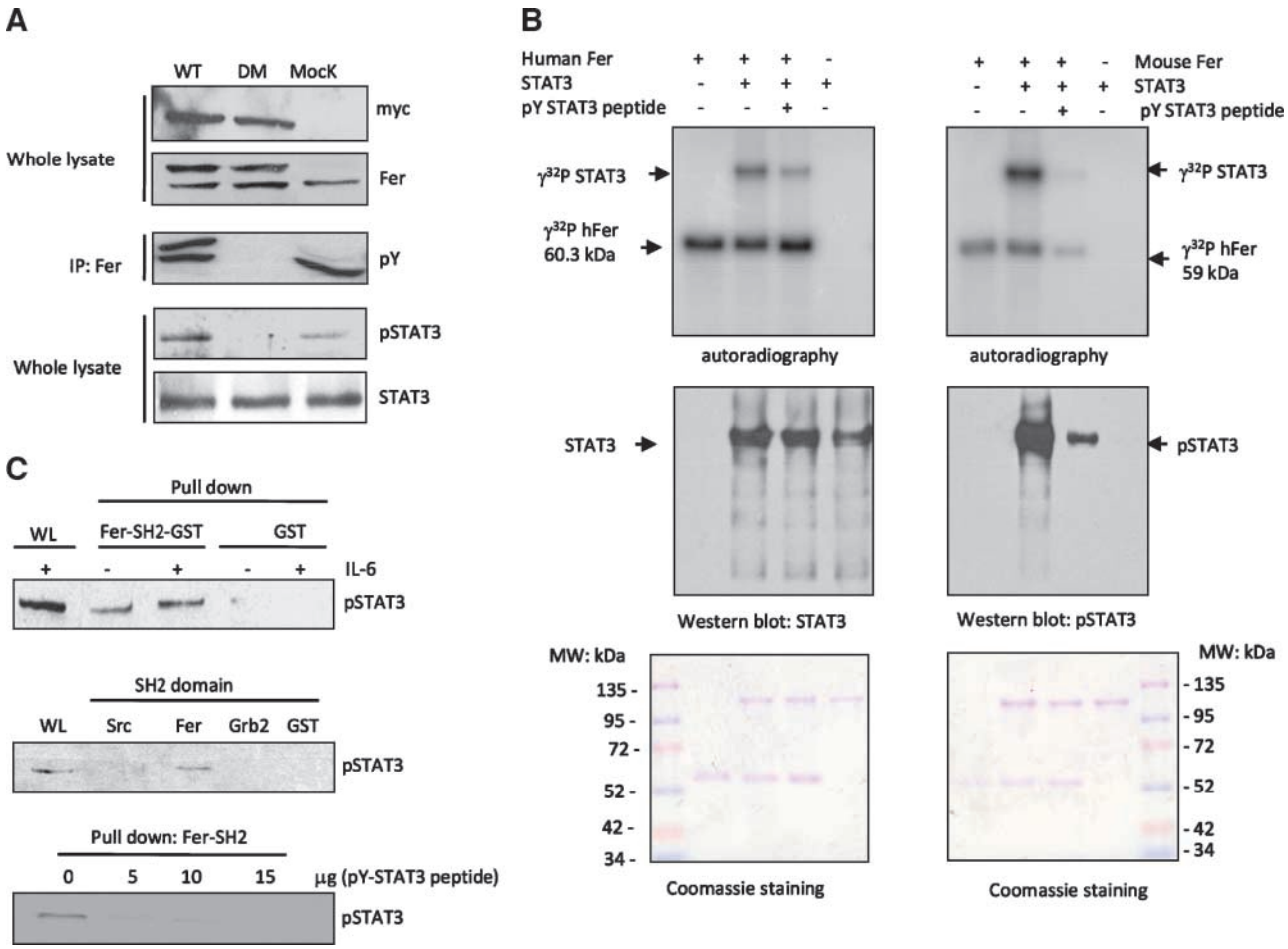


**FIGURE 3.** STAT3 is a Fer substrate and activated STAT3 interacts with Fer via the Fer-SH2 domain. **A.** DM-Fer abrogates STAT3 phosphorylation. PC-3 cells were transfected with 5 μg of plasmids expressing myc-Fer WT and myc-Fer$_{K592R-Y719P}$ DM. Top, 48 h after transfection, cell lysates were analyzed by Western blotting with myc and Fer antibodies to detect endogenous and ectopic Fer; middle, 750 μg proteins were immunoprecipitated with Fer antibodies and Western blotted using phosphotyrosine antibodies to assess Fer tyrosine phosphorylation; bottom, pSTAT3 was detected by a direct immunoblot using pSTAT3 antibodies, and total STAT3 was used as a control loading in this experiment. **B.** Fer directly phosphorylates STAT3. Purified STAT3 (1 μg) was incubated with 1 μg of active Fer in kinase buffer in the presence of [γ-$^{32}$P]ATP for 30 min at 30°C. Controls with either enzyme or substrate alone were included along with labeled ATP in the reaction mixture, as well as the phospho-Y705–specific STAT3 peptide (5 μg) in complete assays with Fer and STAT3. Top, kinase reactions were stopped by adding Laemmli buffer and resolved by SDS-PAGE. Autoradiography was done using phosphorimager. In duplicate experiments, proteins were transferred on membranes for Western blotting using STAT3 (*middle left*) and pSTAT3 (*middle right*) antibodies. Bottom, they were also stained in gels with Coomassie blue. **C.** Fer interacts with pSTAT3 via the Fer-SH2 domain. Total proteins (750 μg) from PC-3 cells stimulated or not with IL-6 were pulled down using Fer-SH2-GST or a GST control. Top, Western blots were done with pSTAT3 antibodies, second panel, extracts from IL-6–stimulated PC-3 cells were pulled down with SH2 domains of Src, Fer, and Grb2, all fused to GST and the control GST. Lower panels, protein extracts from IL-6–stimulated PC-3 cells were preincubated with the phospho-Y705–specific STAT3 peptide at different concentrations (5-15 μg) before pull down using the Fer-SH2 domain. Western blots were done with pSTAT3 antibodies.

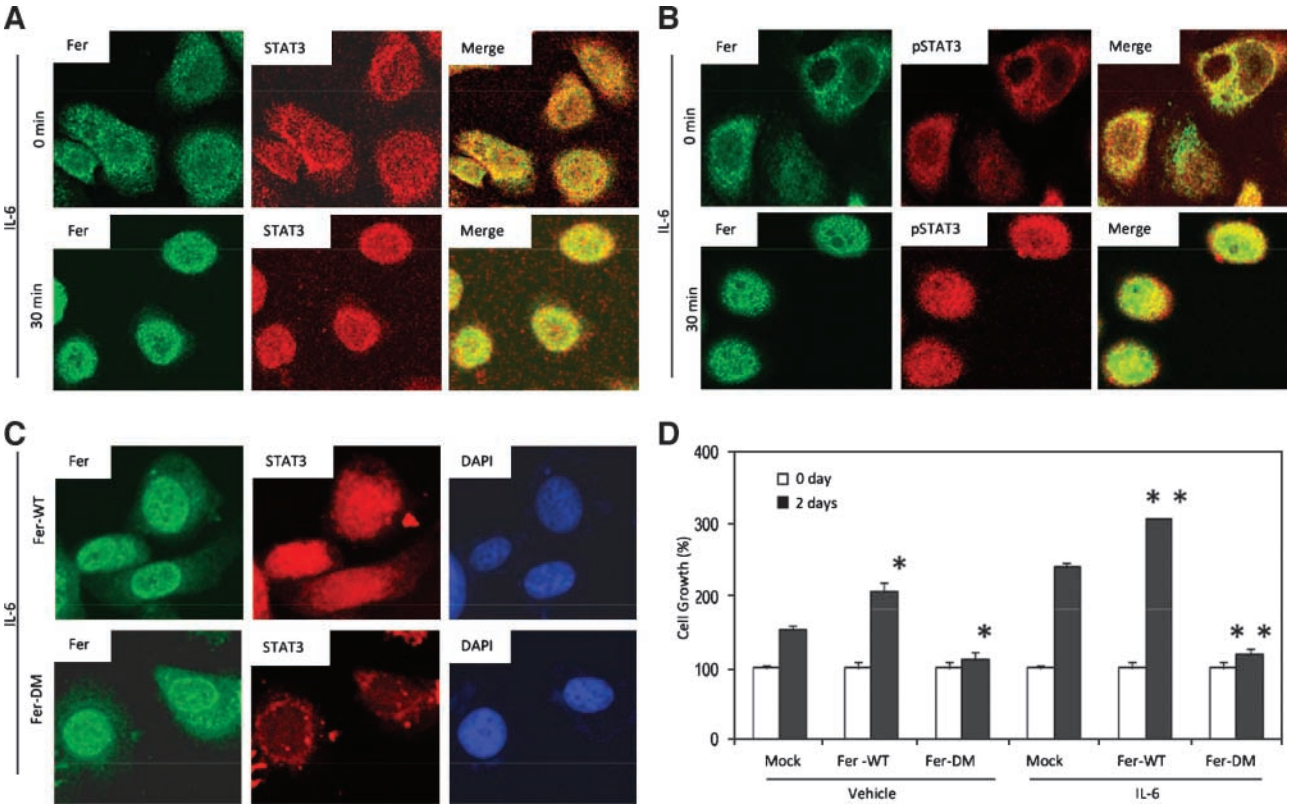


**FIGURE 4.** The IL-6–induced nuclear translocation of Fer and activated STAT3 leading to PC-3 cell growth is under the control of active Fer. **A.** PC-3 cells were exposed to IL-6 for 0 and 30 min. Cells were fixed with paraformaldehyde and double immunofluorescence localizations of Fer and STAT3 were done using Fer (*left*) and STAT3 (*middle*) antibodies. Right, merge images (*green/red*) show colocalization. **B.** Experiments as in **A** showing costaining with Fer and pSTAT3 antibodies. Magnification, ×600. **C** and **D.** PC-3 cells were transfected with plasmids expressing WT-Fer and DM-Fer. Forty-eight hours after transfection, cells were serum starved overnight and exposed to IL-6. In **C**, cells were fixed at $T = 0$ and 30 min of IL-6 for staining with Fer and STAT3 antibodies, with DAPI counterstaining. In **D**, PC-3 cell growth was monitored by MTT assays done at time of IL-6 stimulation (*white columns*, 0 day) and 2 d later (*black columns*). Average values with WT-Fer and DM-Fer were compared with controls (*Mock*) within each series, vehicle (*, $P < 0.05$) and IL-6 stimulated (**, $P < 0.05$).

Bound proteins were analyzed by Western blots using pSTAT3 antibodies. Figure 3C (*top*) shows that pSTAT3 was specifically retained by the Fer-SH2 domain and that the level of bound pSTAT3 was modulated by IL-6. No pSTAT3 protein was detected in pull-down assays done with the GST control or, else, using Grb2 and Src SH2 domains (Fig. 3C, *middle*). Moreover, the addition of increasing amounts of pSTAT3 inhibitor peptide to cell extracts led to a dose-dependent decrease in the amount of pSTAT3 pulled down by the Fer-SH2 domain. These data indicate that the phospho-Y705 motif of STAT3 directly interacts with the Fer and STAT3 SH2 domains and strongly suggest that Fer/pSTAT3 heterodimers coexist with pSTAT3 dimers in prostate cancer cells.

### *Effect of Fer Activation on STAT3 Phosphorylation, Nuclear Translocation, and Cell Growth*

Fer and pSTAT3 are present in both the cytoplasm and nucleus on prostate cancer cells. Thus, we next investigated if IL-6 was able to facilitate the nuclear translocation of Fer along with pSTAT3. Figure 4 shows the immunofluorescence of PC-3 cells treated with IL-6 for 30 minutes, fixed, and immunostained to detect Fer, STAT3, and pSTAT3 by confocal microscopy. In the absence of IL-6 (Fig. 4A), Fer and STAT3 showed a diffuse staining with cytoplasmic and nuclear localization. Furthermore, both proteins colocalized (merge images), a finding in support of immunoprecipitation studies showing that Fer and STAT3 interact (Fig. 4A, *top*). Interestingly, 30 minutes after IL-6 treatment, both Fer and STAT3 had translocated in the nucleus and complexes were colocalized in merge images (Fig. 4A, *bottom*). Staining with pSTAT3 antibodies (Fig. 4B) revealed a faint pSTAT3 staining in the cytoplasm of nonstimulated cells, which may reflect the autocrine production of IL-6. The pSTAT3 signal became intense after IL-6 exposure and was exclusively nuclear. Merge images showed colocalization of pSTAT3 and Fer, primarily in the cytoplasm of nonstimulated cells and in the nucleus after IL-6 treatment. These findings do not only confirm the powerful activity of IL-6 on STAT3 activation and nuclear translocation in PC-3 cells but also show the partnership role of Fer with STAT3 and pSTAT3 in the cytoplasm and, more importantly, accompanying pSTAT3 in the nucleus of prostate cancer cells. Furthermore, we tested the ability of Fer activation on STAT3 nuclear translocation, which is a readout of STAT3 phosphorylation by immunofluorescence (Fig. 4C). In PC-3 cells transfected with WT-Fer and exposed to IL-6, we found

that STAT3 was translocated to the nucleus. However, in cells transfected with DM-Fer and exposed to IL-6, STAT3 showed a perinuclear localization without staining in the nucleus (Fig. 4C). These results point out the importance of Fer activity on STAT3 nuclear localization and STAT3 phosphorylation. To corroborate these results, we did cell growth assays [3-(4,5-dimethylthiazol-2-yl)-2,5-diphenyltetrazolium bromide (MTT)] and found that DM-Fer compromised prostate cancer cell growth (Fig. 4D), thereby highlighting the importance of Fer activation and potential consequences on downstream effectors such as STAT3 phosphorylation and cell growth.

### *Effect of Fer Expression on STAT3 Phosphorylation and Cell Growth*

Fer was reported to control STAT3 activation in COS cells (18). As we showed above by *in vitro* assays, Fer may do so directly. To better investigate the role of Fer in STAT3 tyrosine phosphorylation in prostate cancer cells, a siRNA approach was used to silence Fer expression. As analyzed by real-time PCR, Fer siRNA sequences 1 and 2 reduced Fer mRNA levels by 80% and 65%, respectively, in comparison with the control sequence (Fig. 5A). Consistent with data of Fig. 1A (*bottom*), the siRNA approach largely reduced Fer protein levels, as detected with Fer antibodies in Western blots and without effects on the Fer partner, STAT3 (Fig. 5B, *left*). Moreover, the down-regulation of Fer dramatically reduced STAT3 tyrosine phosphorylation in IL-6–stimulated cells (Fig. 5B, *right*) and had no effect on the housekeeping protein actin. This was detected by Western blots and also by the almost complete loss of the pSTAT3 immunofluorescent signal in the nucleus of PC-3 cells exposed to IL-6 (Fig. 5C, *top*). However, STAT3 down-regulation using siRNA markedly reduced STAT3 expression but did not affect Fer nuclear translocation (Fig. 5C, *bottom*). These observations imply that STAT3 is not essential for IL-6–driven Fer nuclear translocation in PC-3 cells. To support our results on the effect of Fer down-regulation on STAT3 phosphorylation and nuclear translocation, cell growth assays were conducted. Results of MTT assays showed that Fer down-regulation by siRNA reduced PC-3 cell growth compared with cells treated with siRNA control and also abrogated the growth-stimulatory effect of IL-6 (Fig. 5D).

The functional relationship between Fer and PC-3 cell growth was further substantiated by reexpressing recombinant canine WT-Fer after Fer knockdown using siRNA. Figure 5E (*bottom*) similarly reproduces Fer siRNA effects within this time frame and illustrates the ability of WT-Fer to reverse the effect of Fer siRNA and to increase PC-3 cell growth. This was shown in the presence or absence of IL-6. Taken together, Fer expression seems critical for IL-6–mediated STAT3 activation by phosphorylation and PC-3 cell responsiveness resulting in growth. Altogether, these findings indicate that the expression of Fer kinase is essential for IL-6 signaling via activated STAT3 and controlling prostate cancer cell growth.

### *Fer Regulates IL-6–Mediated STAT3 Transcriptional Activity*

To further assess consequences of modulating Fer activation/expression on IL-6 signaling, STAT3 transcriptional activity was analyzed in relation with the extent of Fer activation (WT and DM) or expression (control siRNA and Fer siRNA). STAT3 transactivation assays were done using PC-3 cells transiently transfected with a luciferase reporter plasmid regulated by the STAT3 enhancer-promoter region in the presence or absence of increasing amounts of exogenous WT-Fer (Fig. 6). IL-6 treatment increased STAT3 reporter gene expression by 10-fold. The overexpression of WT-Fer further increased IL-6–stimulated transcriptional activity of STAT3 in a dose-dependent manner, yielding an overall 20-fold increase over empty vector and absence of IL-6 (Fig. 6A). In contrast, DM-Fer decreased the transactivation of IL-6–regulated STAT3 reporter in a dose-dependent manner, further supporting the role for Fer activation in STAT3 transactivation (Fig. 6B). We next analyzed the effect of Fer knockdown on STAT3 transactivation using Fer siRNA 1 and 2. Fer knockdown affected dramatically STAT3 transcriptional activity in the presence of IL-6 (Fig. 6C). The decrease after Fer knockdown was dose dependent but sequence independent. These results indicate that expression and activation of the Fer is a key for IL-6–mediated STAT3 phosphorylation and transcriptional activation.

Collectively, these results illustrate a novel mechanism by which the Fer tyrosine kinase directly contributes to IL-6–mediated activation of STAT3 phosphorylation and nuclear translocation to regulate STAT3 transcriptional activation and promote growth in prostate cancer.

## Discussion

Cytokine signaling has become increasingly more complex than initially thought, with cytokine action on cell types other than hematopoietic and involving not only classic members of the JAK family (31). Indeed, the present investigation provides insight on a novel mechanism by which Fer tyrosine kinase largely contributes to the IL-6 pathway in the human PC-3 cell line, mimicking the androgen-independent stage of prostate cancer (1, 32) and potentially controlling STAT3 activation *in situ* in tumors. Moreover, several observations on Fer represent novel findings that may apply to IL-6 signaling in general and/or other cytokines and model systems.

The specific nature of Fer polyclonal antibodies produced against a Fer-GST fusion protein was first ascertained. It was shown by biochemical means, immunofluorescence, and immunohistochemistry that Fer antibodies specifically detected endogenous Fer in prostate cancer tissues and cells as well as recombinant myc-tagged Fer in cell lines. In addition, the protein was present in the cytoplasm and the nucleus of prostate cancer cells, in agreement with earlier fractionation studies (11). In support of the literature (31, 33, 34), IL-6 stimulation of PC-3 cell growth was confirmed and shown to occur through tyrosine phosphorylation of STAT3. Our observations on Fer strongly suggest that Fer fulfills key functions in IL-6–mediated PC-3 cell growth. Indeed, Fer seemed as a predominant protein kinase of this pathway that binds gp130, activates STAT3, escorts this transcription factor in its ultimate site of action in the nucleus, and controls STAT3 transcriptional activity. Indeed, IL-6 induced the formation of gp130 and STAT3 complexes with Fer in parallel to the activation of

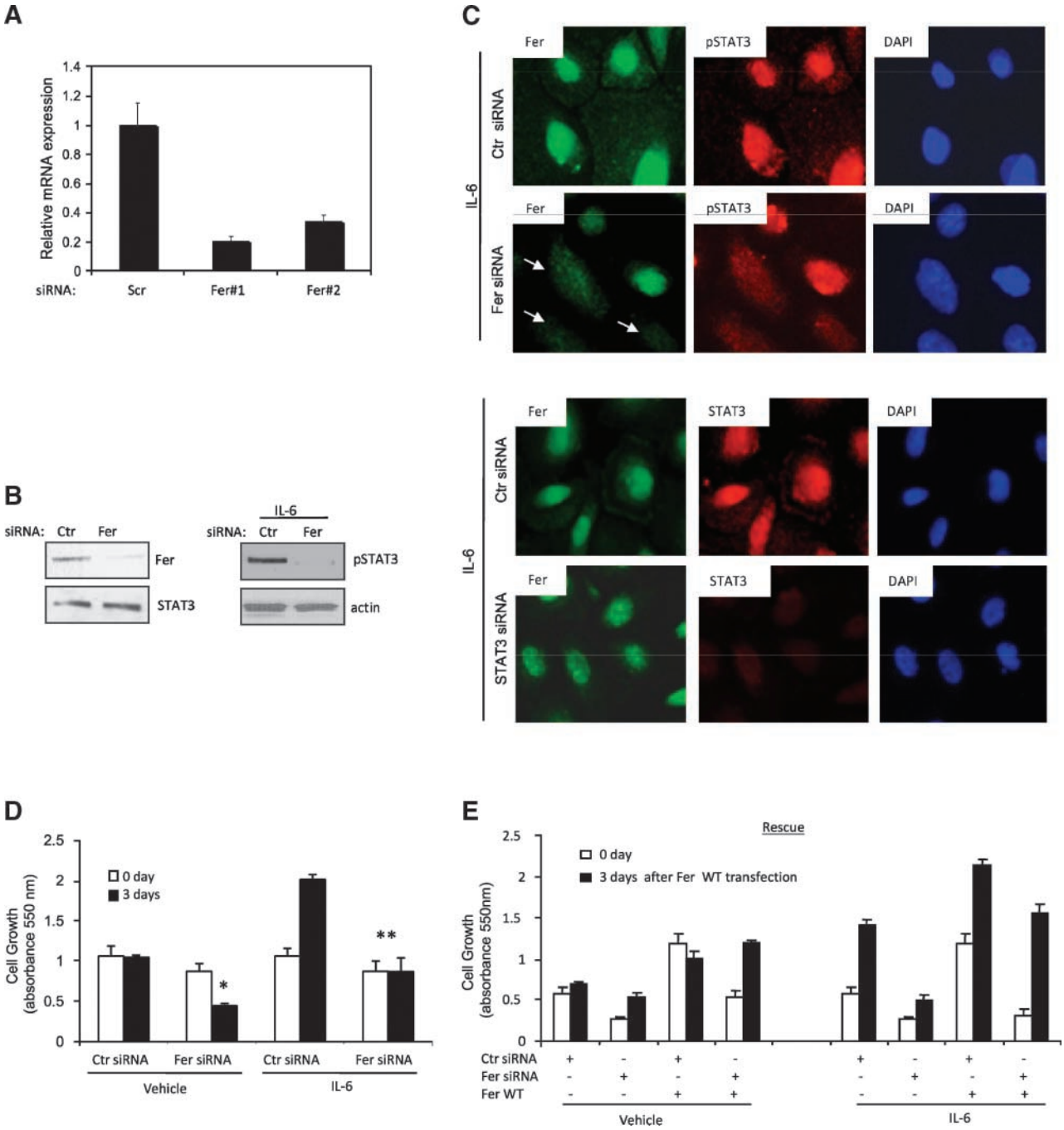


**FIGURE 5.** Fer knockdown abrogates STAT3 phosphorylation and prostate cancer cell growth in response to IL-6. **A.** siRNA *fer* down-regulates Fer at mRNA level. PC-3 cells were transfected with siRNA targeting *fer* with sequences 1 and 2 together with an unrelated sequence used as a siRNA control (*Ctl*) for transfection. Seventy-two hours later, RNA was extracted to do real-time PCR, as described in Materials and Methods. Values are reported relative to the control siRNA. **B.** siRNA *fer* down-regulates Fer expression at protein level and inhibits IL-6–induced STAT3 tyrosine phosphorylation. PC-3 cells were transfected with siRNA *fer* sequence 1 and the control sequence as in **A.** Left, proteins (30 μg) were used for Western blot to detect Fer and STAT3. PC-3 cells were transfected with siRNA *fer* sequence 1 or control sequence as above. After 72 h, cells were serum starved overnight and stimulated with IL-6 for 60 min to analyze pSTAT3 by direct Western blotting (50 μg proteins). Actin was used as a loading control. **C.** *fer* knockdown inhibits the IL-6–induced nuclear accumulation of activated STAT3, whereas STAT3 knockdown does not prevent nuclear transfer of Fer. PC-3 cells were transfected with siRNA *fer* sequence 1, siRNA *stat3* sequence 2, and control sequence as above. Seventy-two hours after transfection, cells were serum starved overnight and stimulated with 100 ng/mL IL-6 for 30 min. They were fixed and immunostained to detect Fer, pSTAT3 (*top*), and STAT3 (*bottom*) and counterstained with DAPI. **D.** Cells transfected with siRNA *fer* sequence 1 and control sequence were stimulated with 100 ng/mL IL-6 as above or vehicle and further cultured. MTT assays were done at time of IL-6 stimulation (*white columns*, 0 day) and 3 d later (*black columns*) to assess growth. Average values with siRNA *fer* were compared with siRNA control (*Ctl*) within each series, vehicle (*, $P < 0.05$) and IL-6 stimulated (**, $P < 0.05$). **E.** For rescue in bottom panel, cells were transfected with siRNA *fer* sequence 1 and control sequence. On the second day, they were transfected with canine WT-Fer cDNA or empty vector (as in Fig. 4) and cultured for 24 h before serum starvation overnight. MTT assays were done on day 4 ($T = 0$) before addition of IL-6 and after an additional 48 h of culture ($T = 3$ d after transfection with WT-Fer).

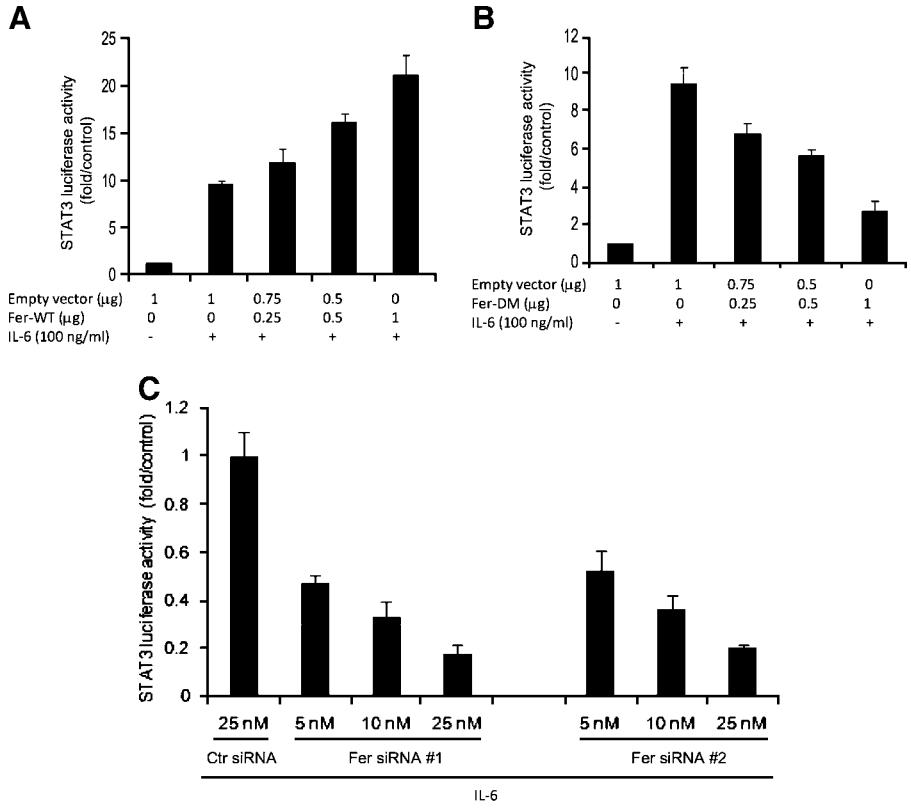


**FIGURE 6.** Effect of Fer activation and expression on STAT3 transcriptional activity in response to IL-6. PC-3 cells were transiently cotransfected with 1 μg of STAT3-luciferase together with various concentrations (0, 0.25, 0.5, and 1 μg/well) of *fer* cDNA, WT (**A**) or DM (**B**). Total amount of plasmid DNA transfected was normalized to 2 μg/well using empty vector pcDNA3.1. Twenty-four hours after transfection, cells were stimulated with 100 ng/mL IL-6 for 24 h or vehicle to determine luciferase activity. In **C**, PC-3 cells were transfected with various concentrations (5-25 nmol/L) of siRNA *fer* sequences 1 and 2 and 25 nmol/L of the siRNA control (*Ctl*) sequence. Forty-eight hours after transfection, cells were transfected with pLucTKSTAT3 luciferase in parallel with *Renilla*. Twenty-four hours after plasmid transfection, the serum-free medium was replaced with medium containing 100 ng/mL IL-6 for another 24 h. Luciferase activity (in arbitrary light units) is expressed as fold induction.

gp130 and STAT3 (pSTAT3), as detected with pSTAT3 antibodies and also competed for by a phospho-Y705–specific STAT3 inhibitor peptide. The likelihood of a direct physical interaction between Fer and pSTAT3 is supported by the ability of the Fer-SH2 domain to bind pSTAT3, whose levels were increased after IL-6 treatment and reduced in a dose-dependent manner by phospho-Y705–specific STAT3 inhibitor peptide. The fact that pSTAT3 was not retained by SH2 domains of Grb2 and the Src kinase adds specificity to this otherwise unpredictable Fer/pSTAT3 interaction [based on proteomic approaches (35)]. More importantly and in addition to Fer activation, IL-6 regulated Fer intracellular distribution and induced its translocation from the cytoplasm to the nucleus in parallel with STAT3 nuclear translocation. However, the presence of STAT3 was not a prerequisite for IL-6 to drive Fer in the nucleus. Hence, it is worth emphasizing that in PC-3 cells coexpressing Fer and STAT3 in a functional IL-6 signaling pathway, Fer was found in phosphotyrosine-STAT3 nuclear complexes at particularly elevated levels. Taken together, these findings support the implication of Fer in IL-6 signaling up to the nucleus, a novel function that has not been described for JAKs (36) or, else, for Fes in IL-6–stimulated hematopoietic cells (37). A significant observation of the IL-6 signaling pathway was the link between Fer and STAT3 activations shown by modulation of Fer expression and activation in PC-3 cells. Although this is in line with other reports (16, 38), one of the particularly interesting feature was that the overall tyrosine phosphorylation of STAT3, and not only the portion found in Fer complexes, was drastically reduced in PC-3 cells expressing DM-Fer. In support of transfection studies in COS cells (13), these data argue for a major role of Fer in IL-6 signaling and activation of STAT3 in prostate cancer cells. Further support comes from the ability of Fer to directly phosphorylate STAT3 *in vitro* in a reaction also involving Y705. It is worth emphasizing that Fer/STAT3 complexes were evidenced in all human prostate cancer cell lines tested, notably in PRO4 and LN4[3] variants derived from PC-3 cells. This supports a general role of Fer in STAT3 activation in prostate cancer, including in the androgen-sensitive LNCaP model (data not shown), a prostate cancer cell line where IL-6 mimics the action of androgens via cross-talks between AR and STAT3 (39, 40). It is also possible that other cytokines or factors may modulate Fer/STAT3 complexes in prostate cancer cells, as suggested by studies on IFN-γ inhibition of human colon cancer cells (24) and insulin stimulation of myogenic cells where JAKs interact with Fer (19). Hence, Fer formed complexes with gp130, thereby suggesting that Fer may act jointly with JAKs as enzymes expressed in prostate cancer (41) and also known to associate with Fer in other systems (19). Our findings minimize the contribution of other tyrosine kinases in STAT3 activation, notably Fes, which was not detected in prostate cancer cells. They support that Fer exerts its function upstream of STAT3 and possibly up to the nucleus particularly because elevated levels of nuclear Fer/phosphotyrosine-STAT3 complexes were detected after IL-6 stimulation. A strong possibility supported by our findings is that Fer/phosphotyrosine-STAT3 heterodimers coexist with pSTAT3 dimers through physical interactions

[3] Unpublished data.

involving the phospho-Y705 motif of STAT3 and both SH2 domains of Fer and STAT3. In the end, the presence of Fer/phosphotyrosine-STAT3 heterodimers seemed to positively affect further pSTAT3 signaling and transcriptional activity to promote growth. Indeed, our data on Fer expression and activation affecting STAT3 transcriptional activity agree with findings in COS cells (18), showing that by regulating activated STAT3, Fer controls pSTAT3 binding to DNA regulatory sequences.

The physiologic role of Fer and implication in diseases is still elusive. For instance, Fer activity is not essential for embryogenesis and postnatal development (42) and redundancy was proposed. Moreover, transcripts seem to be ubiquitously expressed (43). The protein has not been extensively studied in tissues, but based on data in the adult prostate, some regulation seems to take place in specific cell types. Typically, Fer is barely detectable or at very low levels when the differentiated luminal epithelium predominates in normal or hyperplastic glands (11). On the other hand, Fer protein expression is induced when normal precursor basal cells grow independently of androgens, either in primary culture or in metaplastic dog prostate (11). More importantly, Fer seems to be constitutively expressed in prostate cancer, tissues, and cell lines. Therefore, a more generalized relationship may exist between Fer and growth *in vivo* in different organs, according to hormones, cell phenotypes, and disease state. Earlier attempts to knock down *fer* by stably transfecting PC-3 cells with an antisense *fer* cDNA construct suggest that null Fer PC-3 clones do not survive, whereas reducing Fer levels drastically slows down growth (11). In the present study, it was not possible using Fer siRNA to totally abolish Fer expression as cells would detach if not provided with serum or growth-promoting factors such as IL-6. The expression of *fer* short hairpin RNA through an inducible vector system would be necessary to better clarify the role of Fer in survival of cancer cells and before doing studies in animal models. For instance, beside STAT3, Fer was shown to phosphorylate the TATA modulatory factor (44) and to bind the chromatin (45). This raises the controversial issue of the uniqueness of Fer subcellular distribution in cells, exclusively seen in the nucleus or in the cytoplasm (12, 42, 46) or, else, in both compartments, as shown in prostate cancer cell lines (11) and tissues in the present study. Thus, Fer function may change according not only to cell types but also to localization and interaction with different partners in specific contexts. Recent reports on diverse components of the IL-6 pathway and ranging from IL-6, gp130, to STAT3 and phosphotyrosine-STAT3 in human prostate cancer support the existence of growth-stimulatory loops, particularly characteristic of more advanced or androgen-refractory stages of the disease (47, 48). Based on *in vitro* findings in prostate cancer models (34, 49, 50), we propose that Fer may be a missing effector acting in this pathway, with deregulated expression and/or function in prostate cancer. This is supported by earlier (Western blotting experiments; ref. 11) and present (immunohistochemistry) observations indicating an up-regulated Fer expression in human prostate cancer, as detected in tumor cells of high Gleason score but not in nonmalignant cells within the same sections. Moreover, in subsets of tumors, Fer distribution in the cytoplasm and the nucleus of malignant cells resembled that of pSTAT3 in adjacent sections and correlating with high Gleason score. It is thus tempting to propose that the two molecules may cooperate to favor progression of the disease.

Overall, the present investigation confirms and extends reported findings on the role of Fer in diverse cell models in general and in the cytokine signaling pathway in particular. Our observations support the concept that Fer overexpression, activation, and distribution in the cytoplasm and nucleus of subsets of prostate cancer cells largely contribute to the STAT3 constitutive association with Fer and activation by Fer in these subcellular compartments. Because Fer/STAT3 and pSTAT3 are modulated by IL-6 in parallel with Fer activation and that Fer activity is largely responsible for STAT3 activation and its transcriptional activity in the nucleus, it is very likely that the entire cascade is hyperactivated when cytokine levels increase in patients, thereby favoring growth and progression. Finally, the down-regulation of Fer expression or activation profoundly affects STAT3 activation and STAT3 transcriptional activity and leads to inhibition of prostate cancer cell growth. Therefore, further investigations are justified to exploit Fer as a potential therapeutic target for androgen-independent prostate cancer.

## Materials and Methods

### *Cell Lines, Cell Culture, and Constructs for Transfection*

Human prostate cancer cell lines PC-3, DU145, and LNCaP were purchased from the American Type Culture Collection. The PC-3M cell variants, PRO4 and LN4, were kindly provided by Dr. I. Fidler (M. D. Anderson Cancer Center, Houston, TX). Cells were maintained in RPMI 1640 containing 10% fetal bovine serum and 1% antibiotic/antimycotic (Invitrogen-Life Technologies, Inc.).

Cells were transfected using HiperFect with validated siRNAs designed to target human *fer* with sequence 1 [CAGATAGATCCTAGTACAGAA (SI00287756)] and sequence 2 [CAGAACAACTTAGTAGGATAA (SI02622067)], along with *stat3* with sequence 1 [CAGCCTCTCTGCAGAATTCAA (SI02662338)] and sequence 2 [CAGGCTGGTAATTTATATAAT (SI02662898)], and control nonmammalian sequence [AATTCTCCGAACGTGTCACGT (Alexa Fluor 488, 1022563)], according to the manufacturer's instructions (Qiagen). Cells were also transiently transfected to express recombinant WT-Fer and DM-Fer. For this purpose, the canine *WT-fer* cDNA was subcloned in pcDNA3.1 tagged with myc-6His epitope on COOH-terminal, as previously described (11). The *DM-fer* was generated by mutagenesis to replace $Lys^{591}$ (in ATP-binding site of Fer catalytic domain) by arginine and the regulatory $Tyr^{714}$ by phenylalanine using QuickChange II XL (Site-Directed Mutagenesis kit), according to the manufacturer's instructions (Stratagene).

### *Fer Antibodies*

We previously reported on rabbit polyclonal antibodies raise against a COOH-terminal Fer peptide that detect and immunoprecipitate recombinant myc-tagged Fer and endogenous Fer (94-kDa protein) in extracts from prostate tissues and cells (11). However, in Western blots, other bands were detected by Fer peptide antibodies along with other commercially available Fer peptide antibodies (COOH terminus, Abcam; $NH_2$ terminus, Santa Cruz Biotechnology, Inc. and Chemicon International;

data not shown). Accordingly, new rabbit polyclonal Fer antibodies were generated against a 44-kDa $NH_2$-terminal Fer fusion protein induced in *Escherichia coli* and generated from a 420-bp *Eco*RI-*Eco*RI of the dog fer cDNA (amino acid position 9-146) fused to GST in a pGEX vector (GE Healthcare). Briefly, the Fer fusion protein was induced for 6 h using 0.4 mmol/L isopropyl-L-thio-B-D-galactopyranoside, solubilized with urea, and purified on a Glutathione Sepharose 4B column (GE Healthcare), as recommended by the manufacturer. Purity was assessed by Coomassie staining after electrophoresis (SDS-PAGE), as described below. The GST protein (29 kDa) was similarly produced and used to assess specificity. The immunization protocol (1 mg Fer fusion protein per injection) was as reported earlier (11), following immune response in the antiserum over time by ELISA and until reaching a high titer (over 1 million). IgGs were partially purified from the antiserum and the preimmune rabbit serum (control IgGs) on protein A-Sepharose beads (Invitrogen Corp.).

### *Immunohistochemistry*

A small subset of archived formalin-fixed and paraffin-embedded prostate cancer specimens from patients with clinically advanced disease (transurethral resections) was sectioned (4 μm thick), rehydrated with graded alcohol, and permeabilized with 1% Triton X-100 in PBS for 30 min at room temperature. A 15-min preincubation period at 95°C in 0.01 mol/L sodium citrate buffer (pH 6.0) was included as an antigen retrieval step. It was followed by a 30-min incubation period with 3% hydrogen peroxide in PBS-methanol (1:1) to quench endogenous peroxidase activity. After three washes (5 min with PBS), sections were preincubated with a blocking solution (10% horse serum; Zymed Labs, Inc.) for 30 min to prevent nonspecific staining and next incubated overnight at 4°C with primary antibodies: the above purified Fer antibodies, STAT3, and pSTAT3 (Cell Signaling) in PBS containing 0.1% bovine serum albumin. After three more washes, sections were incubated with biotinylated secondary antibodies (goat anti-rabbit IgGs) and streptavidin-peroxidase conjugate (both from Zymed Labs) to amplify the signal. The staining was revealed within 2 min after addition of 20 μL of 30% hydrogen peroxide in a PBS solution containing 0.006% 3,3′-diaminobenzidine tetrahydrochloride (Sigma-Aldrich Canada Ltd.). Sections were counterstained with hematoxylin, dehydrated, and mounted. Controls included sections incubated without primary antibodies or, else, using preimmune rabbit IgGs or Fer antibodies (4 μg) that had been preincubated with either the Fer fusion protein (antigen) or GST (each at 5 μg/mL).

The relative Fer and pSTAT3 staining intensity and intracellular distribution (%) were assessed blindly to the identity of sections by two independent observers. Grading values represent a consensus on a scale of signal intensity ranging from negative (0) to weak (+), moderate (++), and strong (+++). Data were analyzed using GraphPad Prism version 5.0 software[4] with $\chi^2$ and Kruskal-Wallis followed by Dunn's multiple comparison tests.

[4] http://www.graphpad.com

### *Western Blotting and Immunoprecipitation*

Cells were washed with ice-cold PBS containing 1 mmol/L sodium vanadate and proteins were extracted using radioimmunoprecipitation assay buffer [20 mmol/L Tris-HCl (pH 7.4), 150 mmol/L NaCl, 1 mmol/L sodium vanadate, 1% NP40, 10 μg/mL aprotinin, 10 μg/mL leupeptin]. Proteins were next clarified by centrifugation (14,000 × *g* for 5 min), assayed using the Bradford method (51), and used for direct Western blotting. Membranes were incubated with primary antibodies for 1 h at room temperature to detect Fer (as described above), myc (Invitrogen), gp130 (Santa Cruz Biotechnology), and phosphotyrosine (Cell signaling) or overnight at 4°C for STAT3 and pSTAT3. Peroxidase-conjugated secondary antibodies (Santa Cruz Biotechnology) were used for detection with enhanced chemiluminescence reagent (Amersham Biosciences).

For immunoprecipitation, total proteins (750 μg) were precleared with protein G-Sepharose (Invitrogen-Life Technologies) for 1 h at 4°C and incubated with 2 μg of anti-Fer, anti-STAT3T, phosphotyrosine antibodies, or IgG as a control overnight at 4°C. Immune complexes were recovered with protein G-Sepharose for 2 h and then washed with radioimmunoprecipitation assay buffer at least three times, centrifuged, submitted to SDS-PAGE in 10% acrylamide gels, unless otherwise stated, and Western blotted as indicated.

### *Pull-Down Assays*

A construct of the Fer-SH2 domain (residues 451-564) was generated as a fusion protein with GST and subcloned in the pGEX-3-T vector (Promega). The fusion protein was induced in bacteria at 30°C with 0.4 mmol/L isopropyl-L-thio-B-D-galactopyranoside for 4 h. Proteins were extracted by sonication in PBS followed by solubilization in 0.1% of Triton X-100 for 30 min at room temperature. Fusion proteins were purified and analyzed in gels by Coomassie staining, as described above for the Fer $NH_2$-terminal fusion protein.

For pull down, PC-3 proteins (750 μg) were incubated with 10 μg Fer-SH2 fusion protein, SH2 domains of Grb2 and Src (kindly provided by Dr. G. Pelletier, McGill University), or control GST [15 μg normalized for size (52) for 1 h at room temperature]. In some instances, a phospho-Y705–specific STAT3 peptide (5-15 μg; Calbiochem) was added 5 min before pull down. Glutathione Sepharose beads were added and complexes were recovered by centrifugation. Pellets were washed thrice with PBS and submitted to Western blotting using pSTAT3 antibodies.

### In vitro *Kinase Assays*

GST-tagged recombinant Fer kinases (catalytic domain), human (Invitrogen) and mouse (SignalChem), were used to phosphorylate human recombinant STAT3 (GST fusion proteins; SignalChem) *in vitro*. Assays consisted in 1 μg each of enzyme (Fer) and substrate (STAT3) in phosphorylation buffer containing 25 mmol/L Tris-HCl (pH 7.2), 5 mmol/L β-glycerophosphate, 10 mmol/L $MgCl_2$, 0.5 mmol/L EGTA, 200 μmol/L ATP, 0.01% Triton X-100, and 0.5 mmol/L sodium vanadate. Fresh DTT (2.5 mmol/L) was added and [$\gamma$-$^{32}$P]ATP (11.4 μL or 0.829 MBq/assay; specific activity; 111 TBq/mmol; Perkin-Elmer) to start the reaction (total volume, 40 μL).

Controls with either enzyme or substrate alone were included along with labeled ATP in the reaction mixture, as well as the phospho-Y705–specific STAT3 peptide (5 μg) in complete assays with Fer and STAT3. After 30-min incubation at 30°C, tubes were cooled on ice for 10 min before adding Laemmli buffer (5×; 50 μL total volume) and boiling. Samples were submitted to SDS-PAGE in duplicate gels. Radiolabeled bands were detected after 3 h of exposure using a phosphorimager equipped with ImageQuant (version 5.0) or, else, by an overnight autoradiography of X-ray films at room temperature. Proteins were transferred on membranes for Western blotting using STAT3 and pSTAT3 antibodies. They were also stained in gels with Coomassie blue.

### *Immunofluorescence*

Cells cultured in eight-well plastic chambers were washed on ice with cold PBS containing 1 mmol/L sodium vanadate and fixed with 3.7% paraformaldehyde. This was followed by incubations with 50 mmol/L $NH_4Cl$ (10 min), 0.5% Triton X-100 in PBS (5 min), and 0.5% bovine serum albumin-PBS solution (10 min) before incubation with either Fer, STAT3, or pSTAT3 antibodies for 4 h. Immunofluorescence was revealed using anti-rabbit or anti-mouse antibodies coupled to FITC (Alexa Fluor 488) or rhodamine (CY3; Invitrogen). 4′,6-Diamidino-2-phenylindole (DAPI) was used to stain the nuclei. Photomicrographs were taken with a Zeiss LSM5 Pascal confocal microscope (Carl Zeiss Canada Ltd.) or with an inverted Olympus IX-81 microscope equipped with a CoolSnap HQ digital camera and the ImagePro+ software (version 5.0.1; Media Cybernetics).

### *Real-time PCR*

Total RNA was extracted using the High Pure RNA Isolation kit (Roche), according to the manufacturer's instructions. The amount of RNA was quantified by the absorbance 260/280 nm ratio. Quality was ascertained by electrophoresis on agarose gels and visualization of 18S and 28S RNA under UV light. For cDNA synthesis, 1 μg RNA was reverse transcribed using Expand Reverse transcriptase (Roche), according to the manufacturer's protocol. Samples (5 μL of cDNA in a 50 μL final volume) were used to quantify levels of fer transcripts by real-time PCR relative to levels of *succinate dehydrogenase* (*SDHA*) used as a reference housekeeping gene (53). PCRs were carried out using validated primers for Fer (QT00029043) and SDHA (QT00059486) with the QuantiTect SYBR Green PCR Master Mix, according to the manufacturer's instructions (Qiagen), in a MyiQ Single-Color Real-Time PCR Detection System (Bio-Rad). Amplification conditions were as follows: 1 cycle of 15 min at 95°C and 40 cycles of 15 s at 94°C, 30 s at 55°C, and 30 s at 72°C. Each sample was run in triplicate for both target and endogenous genes and reproduced at least two more times. Data were normalized to SDHA gene expression and relative mRNA expression was calculated with the $\Delta\Delta_t$ method ($C_T$ comparative). Differences were considered statistically significant at $P$ value of <0.05.

### *Cell Growth*

Growth was monitored by MTT assays (Sigma-Aldrich Canada; ref. 54). PC-3 ($2 \times 10^3$ cells) plated on 96-well plates were cultured in serum-supplemented medium for 48 h and serum starved for 24 h before the addition of IL-6 (PeproTech) at 100 $ng.mL^{-1}$ or vehicle and replaced twice a day. Experiments were repeated thrice with at least triplicate for each experiment. MTT results were analyzed using the GraphPad Prism 4.0, doing one-way ANOVA tests (Bonferroni multiple). Differences were considered statistically significant at a $P$ value of <0.05.

### *STAT3 Transcriptional Activity*

PC-3 cells ($2.5 \times 10^5$) were plated in six-well plates and cotransfected with WT-fer and/or DM-fer cDNAs, together with pLucTKSTAT3 (generous gift from Dr. L. Reptis, Queens University, Kingston, Ontario, Canada), using lipofectin (6 μL/well; Invitrogen). The total amount of plasmid DNA was normalized at 2 μg/well by the addition of empty vector. Twenty-four hours after transfection, the serum-free medium was replaced with medium containing 100 ng/mL IL-6 for another 24 h. For down-regulation experiments, PC-3 cells were transfected twice with control siRNA or Fer siRNA 1 and 2. Forty-eight hours after transfection, cells were transfected with pLucTKSTAT3 luciferase in parallel with *Renilla*. Twenty-four hours after plasmid transfection, the serum-free medium was replaced with medium containing 100 ng/mL IL-6 for another 24 h. Luciferase activity was measured with the Dual-Luciferase Reporter Assay System (Promega) using a microplate luminometer (EG&G Berthold). Reporter assays were normalized to protein concentrations (to discriminate effects on cell viability) and *Renilla* luciferase (to discriminate the efficacy of transfection). Control and values are expressed in arbitrary light units. All experiments were carried out in triplicate wells and repeated thrice.

## Disclosure of Potential Conflicts of Interest

No potential conflicts of interest were disclosed.

## References

1. Messing EM, Manola J, Sarosdy M, Wilding G, Crawford ED, Trump D. Immediate hormonal therapy compared with observation after radical prostatectomy and pelvic lymphadenectomy in men with node-positive prostate cancer. N Engl J Med 1999;341:1781–8.

2. Gleave ME, Bruchovsky N, Moore MJ, Venner P. Prostate cancer: 9. Treatment of advanced disease. CMAJ 1999;160:225–32.

3. Craft N, Shostak Y, Carey M, Sawyers CL. A mechanism for hormone-independent prostate cancer through modulation of androgen receptor signaling by the HER-2/neu tyrosine kinase. Nat Med 1999;5:280–5.

4. Miyake H, Nelson C, Rennie PS, Gleave ME. Overexpression of insulin-like growth factor binding protein-5 helps accelerate progression to androgen-independence in the human prostate LNCaP tumor model through activation of phosphatidylinositol 3′-kinase pathway. Endocrinology 2000;141:2257–65.

5. Feldman BJ, Feldman D. The development of androgen-independent prostate cancer. Nat Rev Cancer 2001;1:34–45.

6. Canil CM, Moore MJ, Winquist E, et al. Randomized phase II study of two doses of gefitinib in hormone-refractory prostate cancer: a trial of the National Cancer Institute of Canada-Clinical Trials Group. J Clin Oncol 2005;23:455–60.

7. Rao K, Goodin S, Levitt MJ, et al. A phase II trial of imatinib mesylate in patients with prostate specific antigen progression after local therapy for prostate cancer. Prostate 2005;62:115–22.

8. Aspenstrom P. A Cdc42 target protein with homology to the non-kinase domain of FER has a potential role in regulating the actin cytoskeleton. Curr Biol 1997;7:479–87.

9. Craig AW, Zirngibl R, Greer P. Disruption of coiled-coil domains in Fer protein-tyrosine kinase abolishes trimerization but not kinase activation. J Biol Chem 1999;274:19934–42.

10. Tsujita K, Suetsugu S, Sasaki N, Furutani M, Oikawa T, Takenawa T. Coordination between the actin cytoskeleton and membrane deformation by a novel membrane tubulation domain of PCH proteins is involved in endocytosis. J Cell Biol 2006;172:269–79.

11. Allard P, Zoubeidi A, Nguyen LT, et al. Links between Fer tyrosine kinase expression levels and prostate cell proliferation. Mol Cell Endocrinol 2000;159: 63–77.

12. Ben-Dor I, Bern O, Tennenbaum T, Nir U. Cell cycle-dependent nuclear accumulation of the p94fer tyrosine kinase is regulated by its $NH_2$ terminus and is affected by kinase domain integrity and ATP binding. Cell Growth Differ 1999; 10:113–29.

13. Hao QL, Heisterkamp N, Groffen J. Isolation and sequence analysis of a novel human tyrosine kinase gene. Mol Cell Biol 1989;9:1587–93.

14. Letwin K, Yee SP, Pawson T. Novel protein-tyrosine kinase cDNAs related to fps/fes and eph cloned using anti-phosphotyrosine antibody. Oncogene 1988;3: 621–7.

15. Pasder O, Shpungin S, Salem Y, et al. Downregulation of Fer induces PP1 activation and cell-cycle arrest in malignant cells. Oncogene 2006;25: 4194–206.

16. Kim L, Wong TW. Growth factor-dependent phosphorylation of the actin-binding protein cortactin is mediated by the cytoplasmic tyrosine kinase FER. J Biol Chem 1998;273:23542–8.

17. Fan L, Di Ciano-Oliveira C, Weed SA, et al. Actin depolymerization-induced tyrosine phosphorylation of cortactin: the role of Fer kinase. Biochem J 2004;380: 581–91.

18. Priel-Halachmi S, Ben-Dor I, Shpungin S, et al. FER kinase activation of Stat3 is determined by the N-terminal sequence. J Biol Chem 2000;275: 28902–10.

19. Taler M, Shpungin S, Salem Y, Malovani H, Pasder O, Nir U. Fer is a downstream effector of insulin and mediates the activation of signal transducer and activator of transcription 3 in myogenic cells. Mol Endocrinol 2003;17: 1580–92.

20. Drachenberg DE, Elgamal AA, Rowbotham R, Peterson M, Murphy GP. Circulating levels of interleukin-6 in patients with hormone refractory prostate cancer. Prostate 1999;41:127–33.

21. Mora LB, Buettner R, Seigne J, et al. Constitutive activation of Stat3 in human prostate tumors and cell lines: direct inhibition of Stat3 signaling induces apoptosis of prostate cancer cells. Cancer Res 2002;62:6659–66.

22. Campbell CL, Jiang Z, Savarese DM, Savarese TM. Increased expression of the interleukin-11 receptor and evidence of STAT3 activation in prostate carcinoma. Am J Pathol 2001;158:25–32.

23. Horinaga M, Okita H, Nakashima J, Kanao K, Sakamoto M, Murai M. Clinical and pathologic significance of activation of signal transducer and activator of transcription 3 in prostate cancer. Urology 2005;66:671–5.

24. Orlovsky K, Theodor L, Malovani H, Chowers Y, Nir U. $\gamma$ Interferon down-regulates Fer and induces its association with inactive Stat3 in colon carcinoma cells. Oncogene 2002;21:4997–5001.

25. Twillie DA, Eisenberger MA, Carducci MA, Hseih WS, Kim WY, Simons JW. Interleukin-6: a candidate mediator of human prostate cancer morbidity. Urology 1995;45:542–9.

26. Wallner L, Dai J, Escara-Wilke J, et al. Inhibition of interleukin-6 with CNTO328, an anti-interleukin-6 monoclonal antibody, inhibits conversion of androgen-dependent prostate cancer to an androgen-independent phenotype in orchiectomized mice. Cancer Res 2006;66:3087–95.

27. Varghese JN, Moritz RL, Lou MZ, et al. Structure of the extracellular domains of the human interleukin-6 receptor $\alpha$-chain. Proc Natl Acad Sci U S A 2002;99:15959–64.

28. Matsuda T, Fukada T, Takahashi-Tezuka M, et al. Activation of Fes tyrosine kinase by gp130, an interleukin-6 family cytokine signal transducer, and their association. J Biol Chem 1995;270:11037–9.

29. Stahl N, Farruggella TJ, Boulton TG, Zhong Z, Darnell JE, Jr., Yancopoulos GD. Choice of STATs and other substrates specified by modular tyrosine-based motifs in cytokine receptors. Science 1995;267:1349–53.

30. Chung TD, Yu JJ, Kong TA, Spiotto MT, Lin JM. Interleukin-6 activates phosphatidylinositol-3 kinase, which inhibits apoptosis in human prostate cancer cell lines. Prostate 2000;42:1–7.

31. Taga T. Gp130, a shared signal transducing receptor component for hematopoietic and neuropoietic cytokines. J Neurochem 1996;67:1–10.

32. Lokeshwar BL, Block NL. Isolation of a prostate carcinoma cell proliferation-inhibiting factor from human seminal plasma and its similarity to transforming growth factor $\beta$. Cancer Res 1992;52:5821–5.

33. Narimatsu M, Nakajima K, Ichiba M, Hirano T. Association of Stat3-dependent transcriptional activation of p19INK4D with IL-6-induced growth arrest. Biochem Biophys Res Commun 1997;238:764–8.

34. Lou W, Ni Z, Dyer K, Tweardy DJ, Gao AC. Interleukin-6 induces prostate cancer cell growth accompanied by activation of stat3 signaling pathway. Prostate 2000;42:239–42.

35. Huang H, Li L, Wu C, et al. Defining the specificity space of the human SRC homology 2 domain. Mol Cell Proteomics 2008;7:768–84.

36. Carver JA, Rekas A, Thorn DC, Wilson MR. Small heat-shock proteins and clusterin: intra- and extracellular molecular chaperones with a common mechanism of action and function? IUBMB Life 2003;55:661–8.

37. Hackenmiller R, Kim J, Feldman RA, Simon MC. Abnormal Stat activation, hematopoietic homeostasis, and innate immunity in c-fes−/− mice. Immunity 2000;13:397–407.

38. Lunter PC, Wiche G. Direct binding of plectin to Fer kinase and negative regulation of its catalytic activity. Biochem Biophys Res Commun 2002;296: 904–10.

39. Ueda T, Bruchovsky N, Sadar MD. Activation of the androgen receptor N-terminal domain by interleukin-6 via MAPK and STAT3 signal transduction pathways. J Biol Chem 2002;277:7076–85.

40. Chen T, Wang LH, Farrar WL. Interleukin 6 activates androgen receptor-mediated gene expression through a signal transducer and activator of transcription 3-dependent pathway in LNCaP prostate cancer cells. Cancer Res 2000;60:2132–5.

41. Chott A, Sun Z, Morganstern D, et al. Tyrosine kinases expressed *in vivo* by human prostate cancer bone marrow metastases and loss of the type 1 insulin-like growth factor receptor. Am J Pathol 1999;155:1271–9.

42. Craig AW, Zirngibl R, Williams K, Cole LA, Greer PA. Mice devoid of fer protein-tyrosine kinase activity are viable and fertile but display reduced cortactin phosphorylation. Mol Cell Biol 2001;21:603–13.

43. Pawson T, Letwin K, Lee T, Hao QL, Heisterkamp N, Groffen J. The FER gene is evolutionarily conserved and encodes a widely expressed member of the FPS/FES protein-tyrosine kinase family. Mol Cell Biol 1989;9:5722–5.

44. Tolcher AW, Chi K, Kuhn J, et al. A phase II, pharmacokinetic, and biological correlative study of oblimersen sodium and docetaxel in patients with hormone-refractory prostate cancer. Clin Cancer Res 2005;11:3854–61.

45. Hao QL, Ferris DK, White G, Heisterkamp N, Groffen J. Nuclear and cytoplasmic location of the FER tyrosine kinase. Mol Cell Biol 1991;11:1180–3.

46. Greer P. Closing in on the biological functions of Fps/Fes and Fer. Nat Rev Mol Cell Biol 2002;3:278–89.

47. Smith PC, Hobisch A, Lin DL, Culig Z, Keller ET. Interleukin-6 and prostate cancer progression. Cytokine Growth Factor Rev 2001;12:33–40.

48. Simard J, Gingras S. Crucial role of cytokines in sex steroid formation in normal and tumoral tissues. Mol Cell Endocrinol 2001;171:25–40.

49. Liu XH, Kirschenbaum A, Lu M, et al. Prostaglandin E(2) stimulates prostatic intraepithelial neoplasia cell growth through activation of the interleukin-6/GP130/STAT-3 signaling pathway. Biochem Biophys Res Commun 2002;290:249–55.

50. Mori S, Murakami-Mori K, Bonavida B. Oncostatin M (OM) promotes the growth of DU 145 human prostate cancer cells, but not PC-3 or LNCaP, through the signaling of the OM specific receptor. Anticancer Res 1999;19:1011–5.

51. Bradford MM. A rapid and sensitive method for the quantitation of microgram quantities of protein utilizing the principle of protein-dye binding. Anal Biochem 1976;72:248–54.

52. Wafa LA, Cheng H, Rao MA, et al. Isolation and identification of L-dopa decarboxylase as a protein that binds to and enhances transcriptional activity of the androgen receptor using the repressed transactivator yeast two-hybrid system. Biochem J 2003;375:373–83.

53. Ohl F, Jung M, Xu C, et al. Gene expression studies in prostate cancer tissue: which reference gene should be selected for normalization? J Mol Med 2005;83: 1014–24.

54. Zellweger T, Miyake H, Cooper S, et al. Antitumor activity of antisense clusterin oligonucleotides is improved *in vitro* and *in vivo* by incorporation of 2′-*O*-(2-methoxy)ethyl chemistry. J Pharmacol Exp Ther 2001;298:934–40.